Eur. Phys. J. C 11, 51–67 (1999)
Digital Object Identifier (DOI) 10.1007/s100529900149

THE EUROPEAN PHYSICAL JOURNAL C

Elastic and quasi-elastic pp scattering in ^{6}LiH and ^{6}LiD targets between 1.1 and 2.4 GeV

J. Ball[1,2], C.E. Allgower[3], M. Beddo[3,a], J. Bystrický[2], M. Combet[1,2], Ph. Demierre[4], G. Durand[2], J.-M. Fontaine[1,2], D. Grosnick[3,b], R. Hess[4†], Z. Janout[5,c], Z.F. Janout[4,d], V.A. Kalinnikov[5], T.E. Kasprzyk[3], B.A. Khachaturov[5], R. Kunne[1,e], F. Lehar[2], A. de Lesquen[2], D. Lopiano[3,f], V.N. Matafonov[5], I.L. Pisarev[5], A.A. Popov[5], A.N. Prokofiev[6], D. Rapin[4], J.-L. Sans[1,g], H.M. Spinka[3], Yu.A. Usov[5], V.V. Vikhrov[6], B. Vuaridel[4], A.A. Zhdanov[6]

[1] Laboratoire National Saturne, CNRS/IN2P3 and CEA/DSM, CEA/Saclay, 91191 Gif sur Yvette Cedex, France
[2] DAPNIA, CEA/Saclay, 91191 Gif sur Yvette Cedex, France
[3] Argonne National Laboratory, HEP Division, 9700 South Cass Avenue, Argonne, IL 60439, USA
[4] DPNC, University of Geneva, 24 quai Ernest-Ansermet, 1211 Geneva 4, Switzerland
[5] Laboratory of Nuclear Problems, JINR, 141980 Dubna, Moscow Region, Russia
[6] Petersburg Nuclear Physics Institute, 188350, Gatchina, Russia

Received: 19 April 1999 / Published online: 14 October 1999

Abstract. A polarized proton beam extracted from SATURNE II, the Saclay polarized target with ^{6}Li compounds, and a CH_2 target were used to measure elastic and quasi-elastic pp spin-dependent observables in the angular region $60° < \theta_{CM} < 105°$. The beam and/or target polarizations were oriented vertically. Accurate pp data for the analyzing power A_{oono}, spin-correlation parameter A_{oonn}, and the polarization transfer K_{onno} were measured at 1.1 GeV. The observables A_{oono} and K_{onno} were determined at six other energies between 1.6 and 2.4 GeV. At 1.6 GeV, A_{oonn} was also obtained. The individual contributions from H, ^{6}Li, and ^{6}LiD were deduced. The CH_2 target provided A_{oono}(pp) results on free hydrogen and on protons in carbon. The elastic and quasi-elastic observables are compared with existing data and with phase-shift analysis predictions.

1 Introduction

The experiment was carried out within the Nucleon–Nucleon Program (NN) at SATURNE II. The aim of the measurements was the comparison of elastic and quasi-elastic spin-dependent observables so as to extend the energy region of proton–neutron data. For this purpose, the new polarizable target materials ^{6}LiD and ^{6}LiH were used, and the scattering of polarized protons on protons and neutrons in ^{6}Li and D was studied. The pp results are presented here, while the following paper contains the np data. An unpolarized CH_2 reference target was positioned behind the main target, and scattering of polarized protons on hydrogen and on bound nucleons in carbon was measured.

The kinetic energy of 1.1 GeV is close to the highest energy of free quasi-monoenergetic polarized neutrons that can be achieved at SATURNE II. There exist complete sets of elastic pp and np observables [1,2,3] as well as the phase-shift analyses (PSA) [2,4,5]. For this reason, the measurements performed at this energy were very accurate. At six other energies, the analyzing power A_{oono}(pp) and the polarization transfer parameter K_{onno}(pp) were measured. At 1.1 and 1.6 GeV the spin-correlation parameter A_{oonn} was also determined.

Section 2 briefly describes the way the observables were extracted from the recorded data. As many items are common for pp, np, and pn observables, the relevant formulas will be omitted in the pn paper. In Sect. 3, we discuss the existing database for pp observables in the measured energy region. Section 4 is devoted to the beam polarimeters. In Sect. 5, improvements related to the Saclay polarized target are treated. Section 6 describes the experimental setup and off-line analysis. The results are presented in Sect. 7; they are compared with the existing data and with fits of the Saclay–Geneva PSA (SG-PSA) at fixed energies [2,4] and with the energy-dependent PSA of the Virginia Polytechnic Institute [5] (VPI-PSA).

Present address:
[a] Data Ventures LLC, Los Alamos, NM 87544, USA
[b] Department of Physics and Astronomy, Valparaiso University, Valparaiso, IN 46383, USA
[c] Faculty of Nuclear Sciences and Physical Engineering, Czech Technical University, Břehová 7, 11519 Prague 1, Czech Republic
[d] Computing Center of the Czech Technical University, Zikova 4, 16635 Prague 6, Czech Republic
[e] Institut de Physique Nucléaire IN2P3, 91400 Orsay, France
[f] 101 Aroyo del Mar Court, Aptos, CA 95003, USA
[g] Centrale Themis, 66121 Targasonne, France
† Deceased

Table 1. Existing spin-dependent $A_{\rm oono}$(pp) = $A_{\rm ooon}$(pp) and $A_{\rm oonn}$(pp) data in the energy region from 1.0 to 2.5 GeV. The meanings of the symbols are: p pol.: accelerated polarized protons; p scat.: protons polarized by scattering; p: unpolarized protons; d pol.: polarized deuterons; Scint.: active scintillating target; PPT: polarized proton target; PDT: polarized deuteron target; LH_2: liquid hydrogen; LD_2: liquid deuterium; BEV: BEVATRON; COS: COSMOTRON; ZGS: Zero-Gradient Synchroton

$T_{\rm kin}$ (GeV)	$\theta_{\rm CM}$ (deg)	Points	Accelerator	Beam	Target	Ref.
			$A_{\rm oono}$ and $A_{\rm ooon}$			
1.00, 1.10	43–87	46	SATURNE II	p pol.	PPT	[11]
1.09–2.39	18–94	80	SATURNE II	p pol.	CH_2	[12]
1.10–2.40	18–98	212	SATURNE II	p pol.	PPT	[12]
1.97–2.49	70–110	87	SATURNE II	p pol.	CH_2	[13]
1.98–2.50	∼40	15	SATURNE II	p pol.	CH_2	[13]
2.16–2.28	19–52	126	SATURNE II	p	PPT	[14]
2.10–2.31	36–52	44	SATURNE II	p pol.	CH_2	[15]
1.15	59–89	15	SATURNE II	d pol.	PPT	[16]
1.80–2.50	58–110	740	SATURNE II	p pol.	PPT	[17]
1.00–1.15	42–82	50	SATURNE II	p pol.	CH_2	[18]
1.00–2.44	3–15	26	SATURNE II	p pol.	Scint.	[19]
1.74	9–108	11	SATURNE I	p	PPT	[20]
1.03, 1.19	14–87	46	SATURNE I	p	PPT	[21]
1.03–2.24	25–88	46	BNL COS.	p	PPT	[22]
1.70	23–37	6	LBL BEV.	p	PPT	[23]
1.04–1.96	23–88	71	CERN-PS	p	PPT	[24]
1.36	11–25	19	ITEP	p pol.	CH_2	[25]
1.03	9–87	6	ANL-ZGS	p pol.	LH_2	[26]
1.27, 2.21	18–119	39	ANL-ZGS	p pol.	PPT	[27]
1.73–2.44	26–97	94	ANL-ZGS	p	PPT	[28]
1.05–2.30	∼38	3	ANL-ZGS	p pol.	LH_2	[29]
1.05–1.97	32–92	37	ANL-ZGS	p pol.	PPT	[30]
1.27, 2.21	33–87	28	ANL-ZGS	p pol.	LD_2	[31]
1.27, 2.21	22–68	26	ANL-ZGS	p pol.	LD_2	[32]
1.00–2.00	∼ 34	64	KEK	p pol.	CH_2	[33]
			$A_{\rm oonn}$			
1.00–1.10	42–87	44	SATURNE II	p pol.	PPT	[11]
1.10–2.40	20–97	207	SATURNE II	p pol.	PPT	[34]
1.80–2.50	58–110	740	SATURNE II	p pol.	PPT	[17]
0.98, 1.19	14–87	25	SATURNE I	p scat.	PPT	[21]
1.27, 2.21	18–119	39	ANL-ZGS	p pol.	PPT	[27]
1.05–2.30	90	3	ANL-ZGS	p pol.	PPT	[29]
1.05–1.97	32–92	37	ANL-ZGS	p pol.	PPT	[30]

Throughout the paper, we use the NN formalism and the four-index notation for observables given in [6]. Between the notation of [5] and that of Halsen–Thomas [7,8] the following relations hold for the dominant observables treated here: $A_{\rm oono} = A_{\rm ooon} = P_{\rm nooo} = P_{\rm onoo} = P$, $A_{\rm oonn} = C_{\rm NN}$, $K_{\rm onno} = K_{\rm noon} = K_{\rm NN}$, $D_{\rm onon} = D_{\rm nono} = D_{\rm NN}$, and $N_{\rm onnn} = N_{\rm nonn} = H_{\rm NNN}$.

2 Determination of observables

The exact formalism for similar experiments was recently described in [9], and only necessary items will be mentioned here. The subscripts of any observable $X_{\rm srbt}$ refer to the polarization states of the scattered, recoil, beam, and target particles, respectively. The polarizations of the incident and target particles in the laboratory system are

Table 2. The analyzing power $A_{\rm oono} = A_{\rm ooon}$ in scattering of polarized protons either on hydrogen in the ^{6}LiH target, or on bound protons in the ^{6}LiD target. The parentheses in ^{6}Li + D (+H) refer to the small amount of H in the ^{6}LiD target. By the subtraction of the hydrogen effect in ^{6}LiH, the contribution of protons in ^{6}Li was deduced. The three sets of the results are independent. Quoted errors are statistical uncertainties. The relative normalization systematic error due to the beam polarization was ±3%

$T_{\rm kin}$ = 1.095 GeV,			$p_{\rm lab}$ = 1.804 GeV/c	
$\theta_{\rm CM}$ (deg)	-t (GeV/c)^2	$A_{\rm oono}$(pp) H	$A_{\rm oono}$(pp) ^{6}Li + D (+ H)	$A_{\rm oono}$(pp) ^{6}Li
50.5	0.374	$+0.398 \pm 0.007$	$+0.413 \pm 0.009$	$+0.346 \pm 0.014$
52.0	0.395	$+0.372 \pm 0.004$	$+0.407 \pm 0.004$	$+0.362 \pm 0.006$
54.0	0.423	$+0.366 \pm 0.004$	$+0.380 \pm 0.003$	$+0.339 \pm 0.005$
56.0	0.453	$+0.360 \pm 0.004$	$+0.358 \pm 0.003$	$+0.320 \pm 0.005$
58.0	0.483	$+0.339 \pm 0.005$	$+0.342 \pm 0.003$	$+0.303 \pm 0.005$
60.0	0.514	$+0.321 \pm 0.004$	$+0.321 \pm 0.004$	$+0.280 \pm 0.005$
62.0	0.545	$+0.291 \pm 0.005$	$+0.303 \pm 0.004$	$+0.280 \pm 0.005$
64.0	0.577	$+0.277 \pm 0.005$	$+0.279 \pm 0.004$	$+0.256 \pm 0.006$
66.0	0.609	$+0.246 \pm 0.005$	$+0.250 \pm 0.004$	$+0.228 \pm 0.006$
68.0	0.625	$+0.212 \pm 0.005$	$+0.230 \pm 0.004$	$+0.217 \pm 0.006$
70.0	0.676	$+0.202 \pm 0.006$	$+0.213 \pm 0.004$	$+0.178 \pm 0.006$
72.0	0.710	$+0.177 \pm 0.006$	$+0.179 \pm 0.004$	$+0.167 \pm 0.007$
74.0	0.744	$+0.140 \pm 0.006$	$+0.164 \pm 0.004$	$+0.161 \pm 0.007$
76.0	0.779	$+0.121 \pm 0.006$	$+0.131 \pm 0.005$	$+0.128 \pm 0.007$
78.0	0.814	$+0.099 \pm 0.006$	$+0.117 \pm 0.005$	$+0.099 \pm 0.007$
80.0	0.849	$+0.075 \pm 0.006$	$+0.096 \pm 0.005$	$+0.098 \pm 0.007$
82.0	0.884	$+0.058 \pm 0.006$	$+0.071 \pm 0.005$	$+0.053 \pm 0.007$
84.0	0.920	$+0.037 \pm 0.007$	$+0.060 \pm 0.005$	$+0.046 \pm 0.007$
86.0	0.956	$+0.031 \pm 0.007$	$+0.031 \pm 0.005$	$+0.050 \pm 0.008$
88.0	0.991	-0.003 ± 0.007	$+0.015 \pm 0.005$	$+0.024 \pm 0.008$
90.0	1.027	-0.020 ± 0.007	$+0.013 \pm 0.006$	$+0.012 \pm 0.009$
91.5	1.054	-0.016 ± 0.010		
91.9	1.061		-0.022 ± 0.007	-0.014 ± 0.011
93.6	1.092		-0.032 ± 0.013	-0.030 ± 0.017

oriented along the basic unit vectors

$$\vec{k}, \qquad \vec{n} = [\vec{k} \times \vec{k}\,'], \qquad \vec{s} = [\vec{n} \times \vec{k}], \tag{2.1}$$

where $\vec{k}$ and $\vec{k}'$ are the beam and scattered particle directions, respectively, and $\vec{n}$ is the normal to the first-scattering plane.

The scattered protons are analyzed in the directions $\vec{k}\,'$, $\vec{n}$, $\vec{s}\,' = [\vec{n} \times \vec{k}\,']$ and the recoil ones in the directions $\vec{k}''$, $\vec{n}$, $\vec{s}\,'' = [\vec{n} \times \vec{k}'']$, where $\vec{k}''$ is oriented along the recoil particle direction.

In the present experiment, the beam and target polarizations ($\vec{P}_{\rm B}$ and $\vec{P}_{\rm T}$) were oriented vertically. Neglecting the small azimuthal angle ϕ acceptance of the apparatus, the vertical direction is parallel or antiparallel to $\vec{n}$ and the scattering plane is horizontal. This means that the most general formula for the correlated nucleon–nucleon scattering cross section Σ, as given in [6], is considerably simplified. Taking into account the generalized Pauli principle, time reversal, and parity conservation, the single scattering term reduces to:

$$\frac{{\rm d}\sigma}{{\rm d}\Omega} = \left(\frac{{\rm d}\sigma}{{\rm d}\Omega}\right)_0 \Big(1 + A_{\rm oono}P_{\rm B} + A_{\rm ooon}P_{\rm T} + A_{\rm oonn}P_{\rm B}P_{\rm T}\Big), \tag{2.2}$$

where $({\rm d}\sigma/{\rm d}\Omega)_0$ is the differential cross section for single scattering of unpolarized incident and target particles. It depends, as well as all observables, on the single-scattering angle $\theta_{\rm CM}$.

The polarization of protons, outgoing from the target, was determined in the second-scattering on a carbon analyzer. The asymmetry in the pC reaction with one out-

Table 2. (continued)

$T_{\rm kin}$ = 1.595 GeV,			$p_{\rm lab}$ = 2.353 GeV/c		
$\theta_{\rm CM}$ (deg)	-t (GeV/c)^2	$A_{\rm oono}$(pp) ^{6}Li + D (+H)	$\theta_{\rm CM}$ (deg)	-t (GeV/c)^2	$A_{\rm oono}$(pp) ^{6}Li + D (+H)
60.1	0.751	$+0.090 \pm 0.009$	82.0	1.288	-0.010 ± 0.008
62.0	0.795	$+0.062 \pm 0.007$	84.0	1.340	-0.002 ± 0.008
64.0	0.841	$+0.052 \pm 0.007$	86.0	1.392	$+0.005 \pm 0.008$
66.0	0.888	$+0.043 \pm 0.006$	88.0	1.444	$+0.013 \pm 0.008$
68.0	0.936	$+0.040 \pm 0.007$	90.0	1.497	-0.011 ± 0.008
70.0	0.984	$+0.019 \pm 0.007$	92.0	1.549	-0.004 ± 0.008
72.0	1.034	$+0.016 \pm 0.007$	94.0.	1.600	-0.004 ± 0.009
74.0	1.084	$+0.024 \pm 0.007$	95.9	1.652	$+0.000 \pm 0.010$
76.0	1.134	$+0.005 \pm 0.008$	97.9	1.702	$+0.014 \pm 0.012$
78.0	1.185	$+0.004 \pm 0.008$	99.8	1.751	-0.006 ± 0.019
80.0	1.237	$+0.021 \pm 0.008$	101.4	1.793	-0.057 ± 0.057

$T_{\rm kin}$ = 1.795 GeV,			$p_{\rm lab}$ = 2.567 GeV/c	
$\theta_{\rm CM}$ (deg)	-t (GeV/c)^2	$A_{\rm oono}$(pp) H	$A_{\rm oono}$(pp) ^{6}Li + D (+ H)	$A_{\rm oono}$(pp) ^{6}Li
61.3	0.876		$+0.040 \pm 0.018$	
63.2	0.925	$+0.105 \pm 0.043$	$+0.051 \pm 0.009$	$+0.092 \pm 0.045$
65.0	0.973	$+0.101 \pm 0.037$	$+0.065 \pm 0.009$	$+0.025 \pm 0.040$
67.0	1.025	$+0.068 \pm 0.029$	$+0.041 \pm 0.009$	$+0.089 \pm 0.039$
69.0	1.080	$+0.065 \pm 0.030$	$+0.050 \pm 0.009$	$+0.094 \pm 0.038$
71.0	1.136	$+0.094 \pm 0.030$	$+0.055 \pm 0.009$	$+0.051 \pm 0.040$
73.0	1.191	$+0.120 \pm 0.030$	$+0.056 \pm 0.009$	$+0.076 \pm 0.040$
75.0	1.248	$+0.013 \pm 0.033$	$+0.045 \pm 0.010$	$+0.029 \pm 0.041$
77.0	1.305	$+0.031 \pm 0.032$	$+0.060 \pm 0.010$	-0.042 ± 0.042
79.0	1.362	$+0.086 \pm 0.035$	$+0.038 \pm 0.010$	$+0.118 \pm 0.044$
81.0	1.421	-0.059 ± 0.035	$+0.042 \pm 0.011$	$+0.100 \pm 0.043$
83.0	1.480	$+0.014 \pm 0.034$	$+0.019 \pm 0.011$	$+0.037 \pm 0.045$
85.0	1.536	$+0.043 \pm 0.034$	$+0.022 \pm 0.010$	$+0.047 \pm 0.045$
87.0	1.596	-0.065 ± 0.032	-0.002 ± 0.010	$+0.001 \pm 0.043$
89.0	1.656	-0.005 ± 0.033	$+0.022 \pm 0.010$	-0.027 ± 0.045
91.0	1.713	$+0.000 \pm 0.035$	-0.007 ± 0.010	-0.041 ± 0.044
93.0	1.771	-0.014 ± 0.035	$+0.014 \pm 0.011$	-0.026 ± 0.046
95.1	1.833	$+0.004 \pm 0.036$	-0.023 ± 0.011	-0.074 ± 0.047
97.0	1.889	-0.051 ± 0.036	-0.024 ± 0.011	$+0.033 \pm 0.046$
99.0	1.949	-0.037 ± 0.035	-0.026 ± 0.011	-0.018 ± 0.047
100.8	1.999	$+0.023 \pm 0.039$	-0.031 ± 0.012	-0.045 ± 0.056
102.8	2.059		$+0.002 \pm 0.019$	-0.052 ± 0.067
104.7	2.111		-0.025 ± 0.033	

Table 2. (continued)

	T_{kin} = 1.895 GeV,		p_{lab} = 2.674 GeV/c	
θ_{CM} (deg)	-t (GeV/c)^2	A_{oono}(pp) H	A_{oono}(pp) ^{6}Li + D (+ H)	A_{oono}(pp) ^{6}Li
61.5	0.930	$+0.080 \pm 0.049$	$+0.068 \pm 0.048$	$+0.060 \pm 0.040$
63.1	0.973	$+0.087 \pm 0.016$	$+0.017 \pm 0.028$	$+0.043 \pm 0.023$
65.0	1.027	$+0.097 \pm 0.016$	$+0.054 \pm 0.026$	$+0.076 \pm 0.021$
66.9	1.082	$+0.100 \pm 0.017$	$+0.105 \pm 0.025$	$+0.075 \pm 0.021$
69.0	1.142	$+0.071 \pm 0.017$	$+0.067 \pm 0.026$	$+0.113 \pm 0.021$
71.0	1.199	$+0.072 \pm 0.016$	$+0.072 \pm 0.026$	$+0.083 \pm 0.021$
73.0	1.258	$+0.086 \pm 0.016$	$+0.110 \pm 0.026$	$+0.063 \pm 0.022$
75.0	1.317	$+0.088 \pm 0.016$	$+0.044 \pm 0.026$	$+0.057 \pm 0.022$
77.0	1.378	$+0.077 \pm 0.017$	$+0.042 \pm 0.027$	$+0.105 \pm 0.023$
79.0	1.438	$+0.082 \pm 0.017$	$+0.061 \pm 0.028$	$+0.086 \pm 0.023$
81.0	1.500	$+0.032 \pm 0.018$	$+0.073 \pm 0.029$	$+0.055 \pm 0.024$
83.0	1.561	$+0.072 \pm 0.017$	-0.052 ± 0.028	$+0.017 \pm 0.024$
85.0	1.623	$+0.040 \pm 0.018$	$+0.053 \pm 0.028$	$+0.046 \pm 0.024$
87.0	1.685	$+0.000 \pm 0.017$	$+0.040 \pm 0.027$	$+0.000 \pm 0.023$
89.0	1.747	-0.020 ± 0.017	-0.023 ± 0.028	$+0.043 \pm 0.024$
91.0	1.809	-0.017 ± 0.017	-0.013 ± 0.029	-0.013 ± 0.024
93.0	1.871	-0.050 ± 0.019	$+0.000 \pm 0.029$	-0.024 ± 0.024
95.1	1.933	-0.045 ± 0.018	-0.030 ± 0.029	-0.042 ± 0.024
97.0	1.994	-0.046 ± 0.018	$+0.007 \pm 0.028$	-0.049 ± 0.024
99.0	2.056	-0.061 ± 0.018	-0.055 ± 0.029	-0.020 ± 0.025
101.0	2.117	-0.081 ± 0.018	-0.087 ± 0.031	-0.002 ± 0.027
102.3	2.157	-0.089 ± 0.044		
102.8	2.173		-0.112 ± 0.043	-0.051 ± 0.032
104.8	2.234		-0.146 ± 0.070	-0.073 ± 0.045

going charged particle was measured. For a given first-scattering angular bin, this asymmetry depends on the proton energy T_2, on the second-scattering angle θ_C, and on the azimuthal angle ϕ_C.

Due to conservation laws and in the absence of a magnetic field between the first- and second-scattering targets, the longitudinal component of singly scattered protons cannot be determined. For any double-scattering experiment cross section, we have

$$\Sigma(P_B, P_T, A_C) = I_C\left((\frac{d\sigma}{d\Omega}) + (\frac{d\sigma}{d\Omega})_0 \; R\right), \quad (2.3)$$

where I_C and A_C are the differential cross section and the analyzing power of the pC reaction, respectively, $d\sigma/d\Omega$ and $(d\sigma/d\Omega)_0$ are defined as in (2.2), and R is the spin-dependent second scattering term. With this setup used, only the recoil proton polarization was analyzed, and the first spin index s was zero. Under the simplified conditions given above, R reduces to

$$R(\mathrm{pp}) = A_C \; \cos\phi_C \left(P_{\mathrm{onoo}} + K_{\mathrm{onno}} P_B + D_{\mathrm{onon}} P_T + N_{\mathrm{onnn}} P_B P_T \right). \quad (2.4)$$

For the measurements with an unpolarized target, the observables containing the target spin index t vanish, and only A_{oono} in (2.2), as well as P_{onoo} and K_{onno} in (2.4) survive.

In the scattering of nonidentical particles, the scattered particle is taken to be the same as the incident beam one. In our case of pn → pn this is the outgoing proton, and the recoil neutron spin index r is zero. The term R(pn) reduces to:

$$R(\mathrm{pn}) = A_C \; \cos\phi_C \left(P_{\mathrm{nooo}} + D_{\mathrm{nono}} P_B + K_{\mathrm{noon}} P_T + M_{\mathrm{nonn}} P_B P_T \right). \quad (2.5)$$

An unpolarized target therefore provides A_{oono}, P_{nooo}, and D_{nono}.

Table 2. (continued)

	$T_{\rm kin}$ = 2.035 GeV,		$p_{\rm lab}$ = 2.822 GeV/c	
$\theta_{\rm CM}$ (deg)	-t (GeV/c)^2	$A_{\rm oono}$(pp) H	$A_{\rm oono}$(pp) ^{6}Li + D (+ H)	$A_{\rm oono}$(pp) ^{6}Li
61.4	0.995	$+0.129 \pm 0.026$	$+0.084 \pm 0.042$	$+0.078 \pm 0.043$
63.0	1.043	$+0.117 \pm 0.017$	$+0.100 \pm 0.026$	$+0.071 \pm 0.025$
65.0	1.102	$+0.159 \pm 0.018$	$+0.108 \pm 0.024$	$+0.097 \pm 0.021$
67.0	1.163	$+0.117 \pm 0.018$	$+0.109 \pm 0.024$	$+0.065 \pm 0.021$
69.0	1.226	$+0.102 \pm 0.019$	$+0.122 \pm 0.025$	$+0.106 \pm 0.021$
71.0	1.288	$+0.145 \pm 0.017$	$+0.055 \pm 0.025$	$+0.079 \pm 0.022$
73.0	1.351	$+0.107 \pm 0.018$	$+0.081 \pm 0.025$	$+0.129 \pm 0.022$
75.0	1.414	$+0.109 \pm 0.018$	$+0.123 \pm 0.026$	$+0.095 \pm 0.023$
77.0	1.480	$+0.107 \pm 0.018$	$+0.084 \pm 0.027$	$+0.104 \pm 0.024$
79.0	1.544	$+0.085 \pm 0.019$	$+0.119 \pm 0.026$	$+0.037 \pm 0.024$
81.0	1.610	$+0.075 \pm 0.020$	$+0.062 \pm 0.028$	$+0.063 \pm 0.024$
83.0	1.677	$+0.074 \pm 0.019$	$+0.068 \pm 0.027$	$+0.070 \pm 0.024$
85.0	1.744	$+0.022 \pm 0.019$	$+0.044 \pm 0.027$	$+0.033 \pm 0.025$
87.0	1.810	$+0.033 \pm 0.019$	$+0.069 \pm 0.027$	$+0.030 \pm 0.024$
89.0	1.876	-0.002 ± 0.019	$+0.031 \pm 0.028$	$+0.022 \pm 0.024$
91.0	1.943	$+0.020 \pm 0.019$	-0.037 ± 0.027	-0.008 ± 0.025
93.0	2.009	-0.031 ± 0.020	$+0.010 \pm 0.028$	$+0.015 \pm 0.025$
95.0	2.076	-0.044 ± 0.020	-0.045 ± 0.028	-0.041 ± 0.025
97.0	2.144	-0.039 ± 0.020	-0.080 ± 0.028	-0.060 ± 0.025
99.0	2.208	-0.068 ± 0.020	-0.081 ± 0.028	-0.070 ± 0.025
101.0	2.274	-0.080 ± 0.020	-0.086 ± 0.029	-0.029 ± 0.026
102.8	2.332	-0.119 ± 0.023	-0.019 ± 0.032	-0.063 ± 0.030
104.9	2.399		-0.033 ± 0.049	-0.070 ± 0.035

In the previous formulas, we assumed $\cos\phi \sim \cos^2\phi \sim 1$. In fact, the ϕ acceptance of our apparatus was $\pm 8°$, whereas $\phi_{\rm C}$ can have any value in the interval 0°–360°. This was taken into account in the calculations. The mean value of $\langle \sin^2 \phi \rangle \sim 0.007$ introduces a negligibly small amount of $A_{\rm ooss}$ into $A_{\rm oonn}$. Due to the ϕ symmetry of the acceptance, $\langle \sin\phi \rangle \sim 0$ and some remaining undesired observables cancel in the measurements.

The deflection of protons in the weak vertical magnetic field of the target holding coil (Sect. 5) conserves the vertical polarization direction. However, the fringe fields may rotate the spins of beam, scattered, and recoil charged particles. This causes small contributions of other observables, but the dominant quantities remain unaffected. The $P_{\rm B}$ contribution, perpendicular to the beam direction, was calculated using the target field map and was smaller than $0.02 \times P_{\rm B}$. The longitudinal component was found to be zero.

The field disturbs the ϕ symmetry of the acceptance. A term $\epsilon(\text{instr.}) \times \sin\phi$, added in (2.2), accounted for this small instrumental effect.

At a given energy, (2.2) provides four relations for two opposite directions of $\vec{P}_{\rm B}$ and $\vec{P}_{\rm T}$, respectively. Only the opposite proton beam polarizations at SATURNE II for the two ion source polarized states were used. In a dedicated experiment [10] it was found that $P_{\rm B} = |P_{\rm B}^+| = |P_{\rm B}^-|$. On the other hand, $|P_{\rm T}^+| \neq |P_{\rm T}^-|$, but each $P_{\rm T}$ was measured by the same apparatus, and a possible normalization error results in a common factor F, which multiplies both $P_{\rm T}^+$ and $P_{\rm T}^-$.

The conservation laws imply $A_{\rm oono} = A_{\rm ooon} = P_{\rm nooo} = P_{\rm onoo} = M_{\rm nonn} = N_{\rm onnn}$; these conditions were used in the data analysis. The observable $K_{\rm onno}$(pp) at the angle $\theta_{\rm CM}$ is equal to $D_{\rm onon}$(pp) at the angle $180° - \theta_{\rm CM}$. However, this condition was not imposed and was used for data presentations in figures only.

3 Existing elastic and quasi-elastic pp data

In Table 1 we give a list of the existing elastic and quasi-elastic $A_{\rm oono} = A_{\rm ooon}$ and $A_{\rm oonn}$ pp data measured between 1.0 and 2.5 GeV [11–34]. They can be compared with the present results.

The data in [17] are preliminary only, but the final results are available and will be published. The data from [33] were measured with an internal target at $\theta_{\rm lab} = 68°$. Accurate $A_{\rm ooon}$ measurements below 2.5 GeV with an un-

Table 2. (continued)

	$T_{\rm kin}$ = 2.095 GeV,		$p_{\rm lab}$ = 2.885 GeV/c	
$\theta_{\rm CM}$ (deg)	-t (GeV/c)^2	$A_{\rm oono}$(pp) H	$A_{\rm oono}$(pp) ^{6}Li + D (+ H)	$A_{\rm oono}$(pp) ^{6}Li
61.1	1.021	$+0.175 \pm 0.026$	$+0.108 \pm 0.022$	
63.0	1.074	$+0.167 \pm 0.021$	$+0.140 \pm 0.014$	$+0.175 \pm 0.029$
65.0	1.135	$+0.193 \pm 0.021$	$+0.152 \pm 0.013$	$+0.121 \pm 0.025$
67.0	1.197	$+0.155 \pm 0.021$	$+0.126 \pm 0.013$	$+0.109 \pm 0.025$
69.0	1.260	$+0.109 \pm 0.023$	$+0.125 \pm 0.013$	$+0.101 \pm 0.025$
71.0	1.326	$+0.136 \pm 0.021$	$+0.146 \pm 0.013$	$+0.081 \pm 0.026$
73.0	1.391	$+0.149 \pm 0.021$	$+0.119 \pm 0.013$	$+0.139 \pm 0.026$
75.0	1.457	$+0.131 \pm 0.022$	$+0.098 \pm 0.014$	$+0.103 \pm 0.027$
77.0	1.523	$+0.130 \pm 0.021$	$+0.109 \pm 0.014$	$+0.140 \pm 0.028$
79.0	1.590	$+0.099 \pm 0.022$	$+0.124 \pm 0.014$	$+0.094 \pm 0.029$
81.0	1.657	$+0.116 \pm 0.023$	$+0.089 \pm 0.014$	$+0.051 \pm 0.030$
83.0	1.727	$+0.133 \pm 0.025$	$+0.077 \pm 0.015$	$+0.078 \pm 0.030$
85.0	1.795	$+0.024 \pm 0.024$	$+0.043 \pm 0.014$	$+0.050 \pm 0.031$
87.0	1.863	$+0.034 \pm 0.024$	$+0.053 \pm 0.014$	$+0.081 \pm 0.031$
89.0	1.931	$+0.008 \pm 0.024$	$+0.018 \pm 0.015$	$+0.015 \pm 0.031$
91.0	2.000	-0.040 ± 0.025	-0.019 ± 0.014	$+0.010 \pm 0.031$
93.0	2.068	-0.086 ± 0.025	-0.045 ± 0.015	-0.027 ± 0.032
95.0	2.137	-0.046 ± 0.027	-0.053 ± 0.015	-0.066 ± 0.031
97.0	2.206	-0.092 ± 0.026	-0.057 ± 0.015	-0.034 ± 0.032
99.0	2.273	-0.122 ± 0.025	-0.121 ± 0.015	-0.127 ± 0.032
101.0	2.341	-0.086 ± 0.026	-0.087 ± 0.015	-0.053 ± 0.033
102.9	2.406	-0.068 ± 0.027	-0.105 ± 0.017	-0.082 ± 0.036

polarized proton beam and a polarized atomic hydrogen jet were recently performed at COSY. The data are not available yet.

The $A_{\rm oono}$ data measured before 1983 were fitted and analyzed in [35]. In the energy region under discussion, the authors observed a considerable difference in the absolute polarization values between the different data sets. Common fits averaging these sets suggested that the data in [23,29,30] be normalized downward by 10%, 8%, and 8%, respectively. The data in [28,32] needed to be normalized upwards by 15% and 12%. PSA fits, including the SATURNE II data, give similar conclusions to those in [35].

In the energy region under discussion, $K_{\rm onno}$(pp) and $D_{\rm onon}$(pp) were measured at SATURNE II from 0.995 to 2.396 GeV at 7 energies [36,37,38], from 1.80 to 2.10 GeV at four energies [39], and between 1.975 and 2.495 GeV at 20 energies [9]. For pure observables, 302 data points were obtained. In other laboratories, one point was measured at 1.90 GeV at the BNL COSMOTRON [40], and three points were determined at 2.205 GeV at the ANL-ZGS [41].

4 Beam polarimeters

The vertical polarization of the extracted proton beam at SATURNE II was flipped at each accelerator spill. The extracted beam polarization was monitored by a beam line polarimeter PL1 [42,43], which had two pairs of kinematically conjugate arms in the horizontal plane and beam intensity monitors in the vertical plane.

Downstream of PL1, the beam passed through three thin windows and through the target of the second beam polarimeter (PL2) before entering the polarized target. The outgoing beam passed through the CH_2 target, which was 10 mm thick and 15 mm in diameter and placed 16 cm downstream from the polarized target.

The PL2 polarimeter, positioned $\sim$ 2.5 m upstream of the polarized target, measured left–right (L–R) and up–down (U–D) scattering asymmetries [42,44]. The absence of a horizontal beam polarization component resulted in a zero U–D asymmetry.

A third polarimeter (PL3), which measured the L–R asymmetry, was positioned 6.54 m downstream of PL2 on a remotely controlled movable table. The PL3 array could move horizontally, perpendicular to the beam axis [39].

The proton beam energy at the PL1 target was the same as the nominal extracted beam energy with a spread

Table 2. (continued)

	$T_{\rm kin}$ = 2.395 GeV,		$p_{\rm lab}$ = 3.199 GeV/c	
$\theta_{\rm CM}$ (deg)	-t (GeV/c)^2	$A_{\rm oono}$(pp) H	$A_{\rm oono}$(pp) ^{6}Li + D (+ H)	$A_{\rm oono}$(pp) ^{6}Li
61.7	1.181	$+0.186 \pm 0.031$	$+0.191 \pm 0.057$	$+0.185 \pm 0.046$
63.0	1.226	$+0.225 \pm 0.015$	$+0.185 \pm 0.032$	$+0.208 \pm 0.025$
65.0	1.297	$+0.253 \pm 0.015$	$+0.214 \pm 0.028$	$+0.203 \pm 0.020$
67.0	1.369	$+0.200 \pm 0.016$	$+0.174 \pm 0.028$	$+0.179 \pm 0.019$
69.0	1.442	$+0.232 \pm 0.016$	$+0.171 \pm 0.029$	$+0.170 \pm 0.020$
70.9	1.513	$+0.211 \pm 0.017$	$+0.209 \pm 0.029$	$+0.126 \pm 0.020$
73.0	1.590	$+0.208 \pm 0.017$	$+0.179 \pm 0.030$	$+0.183 \pm 0.021$
75.0	1.666	$+0.194 \pm 0.016$	$+0.170 \pm 0.030$	$+0.177 \pm 0.022$
77.0	1.741	$+0.174 \pm 0.017$	$+0.180 \pm 0.031$	$+0.126 \pm 0.022$
79.0	1.818	$+0.146 \pm 0.018$	$+0.105 \pm 0.031$	$+0.121 \pm 0.022$
81.0	1.895	$+0.099 \pm 0.018$	$+0.109 \pm 0.032$	$+0.098 \pm 0.023$
83.0	1.973	$+0.070 \pm 0.018$	$+0.078 \pm 0.033$	$+0.085 \pm 0.023$
85.0	2.052	$+0.057 \pm 0.018$	$+0.071 \pm 0.033$	$+0.039 \pm 0.024$
87.0	2.129	$+0.014 \pm 0.018$	$+0.087 \pm 0.034$	$+0.011 \pm 0.024$
89.0	2.207	-0.013 ± 0.019	$+0.004 \pm 0.034$	-0.019 ± 0.024
91.0	2.287	-0.008 ± 0.019	-0.006 ± 0.034	-0.038 ± 0.024
93.0	2.365	-0.043 ± 0.019	-0.034 ± 0.034	-0.059 ± 0.024
95.0	2.443	-0.086 ± 0.019	-0.154 ± 0.034	-0.062 ± 0.023
97.0	2.521	-0.149 ± 0.019	-0.113 ± 0.033	-0.099 ± 0.023
99.0	2.599	-0.141 ± 0.019	-0.122 ± 0.033	-0.077 ± 0.023
101.0	2.676	-0.174 ± 0.018	-0.158 ± 0.033	-0.147 ± 0.023
103.0	2.753	-0.171 ± 0.018	-0.130 ± 0.033	-0.156 ± 0.024
105.0	2.828	-0.206 ± 0.018	-0.123 ± 0.040	-0.164 ± 0.033

smaller than 200 keV. The beam at the polarized target center lost about 5 MeV with respect to the nominal accelerator energy. The beam energy at the CH_2 target was 8 to 9 MeV smaller than the nominal value. The energy spread was $\sim \pm$ 0.4 MeV in the PL1 target, $\sim \pm$ 3.5 MeV in the polarized target, and $\sim \pm$ 0.9 MeV in the CH_2 target. The spread decreased only slightly with increasing energy.

5 Polarized target

The ^{6}LiD material contained protons in ^{6}Li, D, and a small amount of residual hydrogen. The ^{6}Li, D, and H nuclei are polarized in ^{6}LiH and ^{6}LiD targets. It has been observed that ^{6}Li behaves as ^{4}He + D, where only the deuterons are polarized [45]. This decreases the fraction of polarized protons or neutrons in ^{6}Li to 1/3. We have taken $\omega_D = 0.05$ as the probability of the deuteron to be in a D state; this is in agreement with the majority of calculated values [46]. Then the polarizations of protons $P_{\rm p}$ and neutrons $P_{\rm n}$ in deuterons are related to the deuteron polarization $P_{\rm d}$ by $P_{\rm p} = P_{\rm n} = P_{\rm d}$ (1–1.5 ω_D).

For the ^{6}Li compounds to be polarized, paramagnetic centers must be created by electron irradiation of these materials at a temperature close to that of liquid nitrogen. The target polarization obtained in a given magnetic field depends on the irradiation dose, time, precise temperature, and purity of the material. The target polarization measurement by the NMR method is more accurate for ^{6}LiD than for deuterated aliphatic alcohols or deuterated ammonia. Because of the crystalline structure of ^{6}Li compounds, the NMR spectra show simple resonance behavior, similar to that of polarized proton targets with doped butanol or pentanol. The development of this kind of target has been described in [46,47,48].

In the compounds ^{6}LiH and ^{6}LiD, only the polarization of the protons and the deuterons, respectively, was measured. We assume that equal spin temperature conditions were present. This means that the measurement of the polarization of one element enabled us to deduce the polarizations of the others [48].

To separate the effects from ^{6}Li and from D, a calibration with ^{6}LiH is needed. This material has been specially prepared in St. Petersburg (Russia). For the purpose of the present experiment, two new target containers for the Saclay frozen spin target [47] were constructed. Both were

45 mm thick (in the beam direction) and 20 mm in diameter. They were inserted into the same refrigerator. The distance between the container axes was 3.0 cm vertically. One of them contained ^{6}LiD and one ^{6}LiH materials. This construction allowed either of the targets to be polarized and inserted in the beam without the opening of the cryostat. Both targets were polarized in the homogenous magnetic field of 2.5 Tesla. The deuteron polarization buildup time was around 8 hours.

When the maximum polarization was reached, the target was set into the frozen spin mode. Scattering measurements were performed in the magnetic holding field of 0.33 Tesla (at the target center), provided by a vertical superconducting holding coil [47]. Under these conditions, the relaxation time of the targets averaged around 12 days.

The hydrogen polarizations in the ^{6}LiH target at 1.1 GeV were $\sim +27\%$ and $\sim -30\%$, respectively. The deuteron polarizations in ^{6}LiD at 1.1 and 1.6 GeV were $\sim +5\%$ and $\sim -17\%$. Considerably higher P_T values were obtained in different tests [47]. Unfortunately, because of a failure of the electricity, the target polarization was lost and could not be reestablished. At energies between 1.8 and 2.4 GeV the targets were unpolarized.

6 Experimental setup and off-line analysis

The present measurements were carried out through the the Nucleon–Nucleon Program experimental setup. This apparatus is described in detail in [44]. It consisted of a two-arm spectrometer with an analyzing magnet and a neutron counter (NC) hodoscope in the forward arm. The NC hodoscope was preceded by four veto counters, not used for pp events. Each arm was equipped with single scintillation counters and counter hodoscopes. Signals from these counters triggered eight multiwire proportional chambers (MWPC) with three wire planes each.

The pp triggers were selected by the coincidence of charged particles in both arms. The scintillation counters also measured time of flight (TOF). The forward-proton momenta were analyzed by a dipole magnet and by TOF.

The recoil protons were rescattered on a 6-cm-thick carbon analyzer and L–R and U–D rescattering events were recorded by the MWPC. The acceptance of each arm in the laboratory frame was $\sim \pm 4.5°$ vertically and 23° horizontally. The ϕ acceptance of both arms together was limited to $\pm 8°$. Complete tracking was performed for each recorded event. For the first-scattering, this provided the vertex position in the target, scattering, and azimuthal angles θ_1, ϕ_1, θ_2, ϕ_2, the TOF, and the momentum of the forward-charged particle.

For investigation of the elastic events in ^{6}LiH, a cut of $\pm 2.5°$ was applied on $\Delta\theta_{CM}$ and $\Delta\phi$, together with cuts on the vertex position, TOF, and $\Delta p_{scatt.}$ [44]. The quasi-elastic contribution from ^{6}Li and inelastic events were subtracted by use of the wings of the ϕ distribution. The background was $\sim 6\%$.

The same cuts on TOF and $\Delta p_{scatt.}$ were applied for the study of ^{6}LiD and ^{6}Li in ^{6}LiH. The H events in ^{6}LiH were suppressed by removal of the central part of the $\Delta\theta_{CM}$ and $\Delta\phi$ distributions. So that the inelastic contribution would be reduced as much as possible, the cuts in the space $\Delta\theta_{CM}$ and $\Delta\phi$ were enlarged to a circle of radius 10° only. For ^{6}Li in the ^{6}LiH target, this contribution was estimated to be smaller than 2% at 1.1 GeV and less than 7% at 2.4 GeV. For the entire ^{6}LiD target, the inelastic contamination varied from 1% to 4%, respectively. The cryogenic envelope contributed at the level of $\sim 1\%$ to the number of events. It was taken into account as a dilution of the $|P_T|$ value.

The $\Delta\theta_{CM}$ distribution for pp events in the ^{6}LiH target is shown in Fig. 1. It contains a narrow hydrogen peak and the broad and asymmetric distribution from the quasi-elastic pp events in ^{6}Li. Subtracting the events on hydrogen, one obtains the contribution from ^{6}Li. These events are statistically independent of those for elastic pp scattering on H in the same target. Both sets of the data may be used in any data analysis (e.g., PSA).

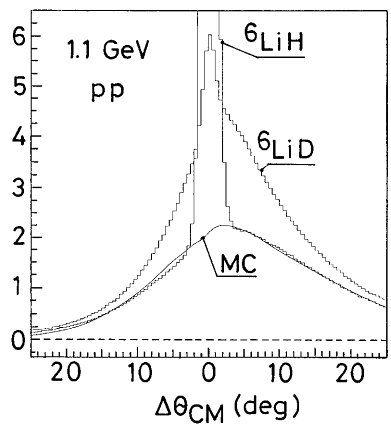

Fig. 1. The normalized $\Delta\theta_{CM}$ distributions of pp events from ^{6}LiH and from ^{6}LiD targets at 1.095 GeV. The small peak in the ^{6}LiD distribution is due to the residual hydrogen. The solid curve was obtained by the Monte Carlo (MC) simulation for quasi-elastic and inelastic events in ^{6}LiH

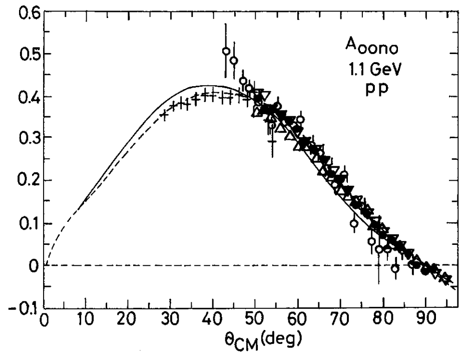

Fig. 2. A_{oono}(pp) energy dependence at 1.095 GeV. •: protons scattered on H in the ^{6}LiH target; ▽: protons on ^{6}Li + D (+H) in the ^{6}LiD target; △: protons on ^{6}Li; ∘: [11]; +: [12]; solid curve: VPI-PSA; dashed curve: SG-PSA

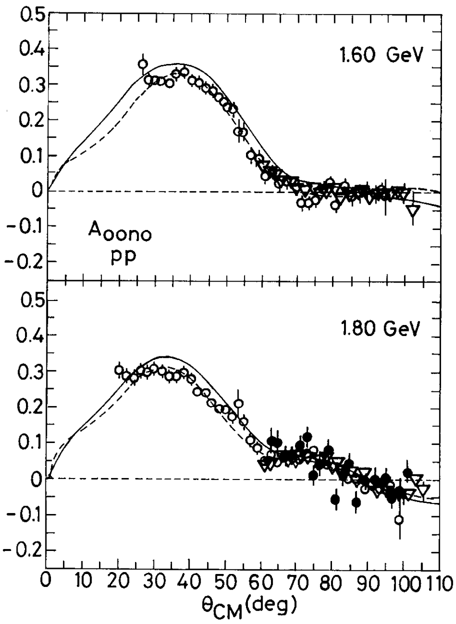

Fig. 3. $A_{\rm oono}$(pp) energy dependence at 1.595 and 1.795 GeV. •: protons scattered on H in the ^{6}LiH target; ▽: protons on ^{6}Li+D (+H) in the ^{6}LiD target; ○: [12]; solid curves: VPI-PSA; dashed curves: SG-PSA

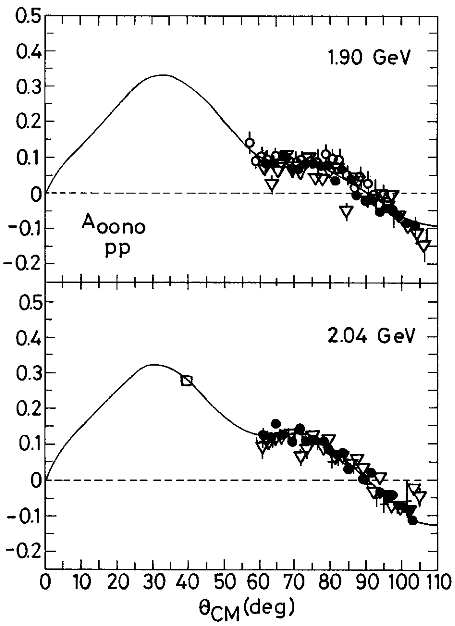

Fig. 4. $A_{\rm oono}$(pp) energy dependence at 1.895 and 2.035 GeV. •: protons scattered on H in the ^{6}LiH target; ▽: protons on ^{6}Li + D (+H) in the ^{6}LiD target; ○: final data at 1.935 GeV from [17]; +: final data at 2.035 GeV [17]; open square: [13]; solid curves: VPI-PSA

Table 3. The pp analyzing power $A_{\rm oono}$ in elastic and quasi-elastic scattering on free and strongly bound protons in the CH_2 target. Quoted errors are statistical uncertainties. All results are independent. The relative normalization systematic error in $P_{\rm B}$ was ±3%

$\theta_{\rm CM}$ (deg)	-t (GeV/c)^2	$A_{\rm oono}$(pp) H	$A_{\rm oono}$(pp) C
$T_{\rm kin}$ = 1.091 GeV, $p_{\rm lab}$ = 1.800 GeV/c			
61.3	0.532	+0.310 ± 0.009	+0.262 ± 0.016
63.1	0.561	+0.291 ± 0.005	+0.227 ± 0.012
65.0	0.591	+0.262 ± 0.005	+0.204 ± 0.012
67.0	0.624	+0.247 ± 0.005	+0.205 ± 0.011
69.0	0.657	+0.208 ± 0.005	+0.197 ± 0.012
70.9	0.689	+0.192 ± 0.006	+0.195 ± 0.013
73.0	0.725	+0.144 ± 0.006	+0.174 ± 0.014
75.0	0.759	+0.141 ± 0.007	+0.119 ± 0.015
77.0	0.794	+0.121 ± 0.008	+0.132 ± 0.017
79.0	0.829	+0.096 ± 0.008	+0.082 ± 0.019
81.0	0.864	+0.075 ± 0.010	+0.076 ± 0.021
83.0	0.899	+0.040 ± 0.011	+0.063 ± 0.024
85.0	0.935	+0.058 ± 0.013	+0.018 ± 0.027
87.0	0.970	+0.031 ± 0.016	+0.071 ± 0.033
89.0	1.006	−0.011 ± 0.019	+0.049 ± 0.044
90.8	1.038	−0.026 ± 0.026	+0.051 ± 0.072
$T_{\rm kin}$ = 1.592 GeV, $p_{\rm lab}$ = 2.350 GeV/c			
71.0	1.007	+0.001 ± 0.037	
76.9	1.155	−0.004 ± 0.021	+0.061 ± 0.035
84.9	1.361	+0.021 ± 0.022	+0.019 ± 0.036
92.9	1.569	+0.033 ± 0.024	+0.013 ± 0.038
98.5	1.714	−0.083 ± 0.040	
$T_{\rm kin}$ = 1.792 GeV, $p_{\rm lab}$ = 2.564 GeV/c			
75.4	1.258	+0.047 ± 0.036	+0.059 ± 0.062
79.0	1.361	+0.055 ± 0.026	−0.025 ± 0.045
83.0	1.476	−0.006 ± 0.028	+0.119 ± 0.044
87.0	1.593	−0.057 ± 0.029	−0.087 ± 0.044
91.0	1.711	+0.003 ± 0.029	
92.8	1.763		−0.051 ± 0.031
95.0	1.828	−0.023 ± 0.030	
99.0	1.944	−0.051 ± 0.030	
99.4	1.956		−0.003 ± 0.042
101.9	2.028	+0.009 ± 0.045	

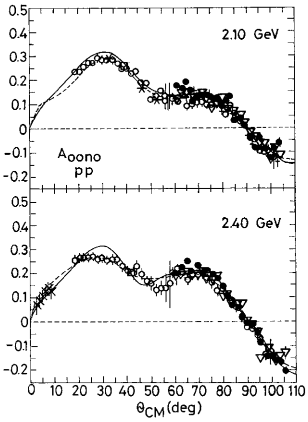

Fig. 5. $A_{\rm oono}$(pp) energy dependence at 2.095 and 2.395 GeV. •: protons scattered on H in the ^{6}LiH target,; ▽: protons on ^{6}Li + D (+H) in the ^{6}LiD target; ∘: [12]; open square: [13]; ⋆: [15]; +: final data at 2.095 GeV from [17]; ×: 2.44 GeV [19]; solid curves: VPI-PSA; dashed curves: SG-PSA

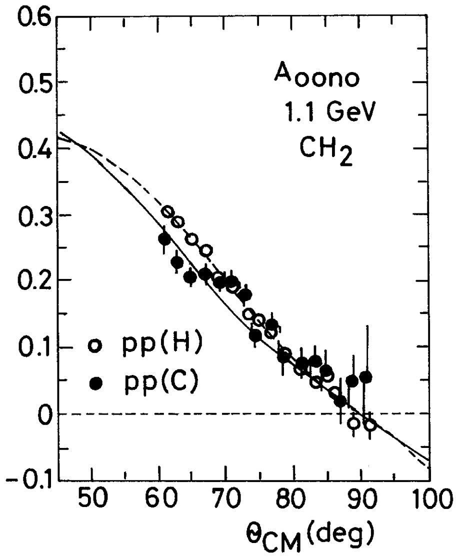

Fig. 6. CH_2 target results at 1.091 GeV. ∘: scattering of protons on H in the CH_2 target; •: pp scattering on protons in C; solid curve: VPI-PSA; dashed curve: SG-PSA

The shape of the $\Delta\theta_{\rm CM}$ distribution for pp, with the ^{6}LiD target used, is shown in the same figure. The small hydrogen peak is due to the residual hydrogen present in this target. The subtraction of ^{6}Li events from ^{6}LiD events gives the quasi-elastic pp effect from D.

In the tables we present the pp elastic data, the quasi-elastic ones from pure ^{6}Li, and the results from the entire ^{6}LiD target. These last data are the most interesting for any future use of ^{6}LiD.

The cuts change the relative trigger contributions from the target components. At 1.1 and 1.6 GeV for pp single scattering in the ^{6}LiD material, we had 52% of effective triggers from ^{6}Li, 44% from D, and 4% from residual hydrogen. At the higher energies, a different target material was used and the hydrogen events represented ∼ 15%.

Table 3. (continued)

$\theta_{\rm CM}$ (deg)	-t (GeV/c)^2	$A_{\rm oono}$(pp) H	$A_{\rm oono}$(pp) C
$T_{\rm kin}$ = 1.892 GeV, $p_{\rm lab}$ = 2.670 GeV/c			
75.4	1.328	$+0.139 \pm 0.053$	$+0.116 \pm 0.095$
79.0	1.436	$+0.087 \pm 0.035$	-0.020 ± 0.065
83.0	1.559	-0.001 ± 0.038	$+0.033 \pm 0.059$
86.9	1.679	$+0.042 \pm 0.038$	$+0.116 \pm 0.057$
91.0	1.806	$+0.019 \pm 0.038$	$+0.069 \pm 0.057$
95.0	1.930	-0.032 ± 0.039	-0.007 ± 0.057
99.0	2.053	-0.051 ± 0.039	-0.109 ± 0.062
102.3	2.153	-0.106 ± 0.050	-0.122 ± 0.148
$T_{\rm kin}$ = 2.032 GeV, $p_{\rm lab}$ = 2.822 GeV/c			
77.8	1.504	$+0.103 \pm 0.039$	$+0.096 \pm 0.097$
85.0	1.740	$+0.036 \pm 0.035$	$+0.077 \pm 0.053$
92.9	2.003	-0.074 ± 0.037	-0.010 ± 0.053
99.8	2.231	-0.028 ± 0.045	-0.074 ± 0.079
$T_{\rm kin}$ = 2.092 GeV, $p_{\rm lab}$ = 2.881 GeV/c			
78.2	1.561	$+0.091 \pm 0.028$	$+0.111 \pm 0.045$
85.0	1.792	-0.014 ± 0.024	$+0.015 \pm 0.034$
93.0	2.066	-0.037 ± 0.026	-0.041 ± 0.035
99.5	2.287	-0.080 ± 0.032	-0.171 ± 0.051
$T_{\rm kin}$ = 2.392 GeV, $p_{\rm lab}$ = 3.195 GeV/c			
78.4	1.793		$+0.122 \pm 0.064$
79.1	1.820	$+0.161 \pm 0.049$	
84.9	2.045	$+0.016 \pm 0.028$	
85.2	2.057		$+0.027 \pm 0.038$
93.1	2.366	-0.112 ± 0.028	-0.065 ± 0.038
98.5	2.576	-0.178 ± 0.045	
99.3	2.607		-0.025 ± 0.067

Since no ^{6}LiH data exist at 1.6 GeV, the individual triggers were obtained by comparing the Monte Carlo acceptances for ^{6}Li and D at 1.1 and 1.6 GeV. We have used the Hulthen distribution $H\ (p_{\rm f})$ of the Fermi momentum $p_{\rm f}$ for bound nucleons in the deuteron:

$$H\ (p_{\rm f}) = \frac{p_{\rm f}^2}{(p_{\rm f}^2+\alpha^2)^2 \times (p_{\rm f}^2+\beta^2)^2} \tag{6.1}$$

with α = 0.045 GeV/c and β = 0.270 GeV/c. We have used a Hulthen-like distribution for ^{6}Li with α = 0.160 GeV/c and β = 0.200 GeV/c, and for carbon with α = 0.225 GeV/c and β = 0.227 GeV/c. These functions describe fairly well all observed distributions. As can be seen for ^{6}Li Monte Carlo simulation in Fig. 1. At 1.1 GeV, the comparison of ^{6}LiH and ^{6}LiD data with the Monte

Table 4. The spin-correlation parameter $A_{\rm oonn}$ in the scattering of polarized protons either on polarized hydrogen in the ^{6}LiH target, or on polarized bound protons in the ^{6}LiD target. The parentheses in ^{6}Li + D (+ H) refer to the small amount of H in the ^{6}LiD target. Quoted errors are statistical uncertainties. The normalization systematic error in $P_{\rm B}$ was ±3%. At 1.095 GeV, $\Delta P_{\rm T}$ = ±4%, while at 1.595 GeV, the accuracy was ±10%

$T_{\rm kin}$ = 1.095 GeV, $p_{\rm lab}$ = 1.804 GeV/c					
$\theta_{\rm CM}$ (deg)	-t $({\rm GeV/c})^2$	$A_{\rm oonn}$(pp) H	$\theta_{\rm CM}$ (deg)	-t $({\rm GeV/c})^2$	$A_{\rm oonn}$(pp) H
50.5	0.374	$+0.545 \pm 0.025$	72.0	0.710	$+0.518 \pm 0.019$
52.0	0.395	$+0.547 \pm 0.012$	74.0	0.744	$+0.527 \pm 0.019$
54.0	0.423	$+0.535 \pm 0.013$	76.0	0.779	$+0.532 \pm 0.019$
56.0	0.453	$+0.536 \pm 0.014$	78.0	0.814	$+0.509 \pm 0.020$
58.0	0.483	$+0.543 \pm 0.015$	80.0	0.849	$+0.549 \pm 0.020$
60.0	0.514	$+0.520 \pm 0.015$	82.0	0.884	$+0.518 \pm 0.022$
62.0	0.545	$+0.523 \pm 0.015$	84.0.	0.920	$+0.531 \pm 0.022$
64.0	0.577	$+0.544 \pm 0.016$	86.0	0.956	$+0.493 \pm 0.022$
66.0	0.609	$+0.525 \pm 0.017$	88.0	0.991	$+0.608 \pm 0.022$
68.0	0.625	$+0.514 \pm 0.017$	90.0	1.027	$+0.536 \pm 0.023$
70.0	0.676	$+0.526 \pm 0.019$	91.5	1.055	$+0.489 \pm 0.033$
$\theta_{\rm CM}$ (deg)	-t $({\rm GeV/c})^2$	$A_{\rm oonn}$(pp) ^{6}Li + D (+ H)	$\theta_{\rm CM}$ (deg)	-t $({\rm GeV/c})^2$	$A_{\rm oonn}$(pp) ^{6}Li + D (+ H)
53.3	0.413	$+0.525 \pm 0.031$	73.0	0.726	$+0.480 \pm 0.039$
57.0	0.467	$+0.557 \pm 0.030$	77.0	0.796	$+0.469 \pm 0.040$
61.0	0.529	$+0.529 \pm 0.031$	81.0	0.866	$+0.528 \pm 0.042$
64.9	0.592	$+0.480 \pm 0.033$	85.0	0.937	$+0.516 \pm 0.044$
68.9	0.658	$+0.476 \pm 0.037$	88.8	1.006	$+0.565 \pm 0.048$
$T_{\rm kin}$ = 1.595 GeV, $p_{\rm lab}$ = 2.353 GeV/c					
$\theta_{\rm CM}$ (deg)	-t $({\rm GeV/c})^2$	$A_{\rm oonn}$(pp) ^{6}Li + D (+H)	$\theta_{\rm CM}$ (deg)	-t $({\rm GeV/c})^2$	$A_{\rm oonn}$(pp) ^{6}Li + D (+H)
61.3	0.778	$+0.471 \pm 0.054$	81.0	1.236	$+0.465 \pm 0.053$
65.0	0.865	$+0.386 \pm 0.043$	85.0	1.340	$+0.465 \pm 0.053$
69.0	0.960	$+0.387 \pm 0.043$	89.0	1.444	$+0.555 \pm 0.053$
72.9	1.058	$+0.422 \pm 0.046$	92.9	1.548	$+0.608 \pm 0.054$
77.0	1.159	$+0.421 \pm 0.051$	96.7	1.648	$+0.458 \pm 0.068$

Carlo simulation is consistent with a shadowing effect of ~ 0.8 on ^{6}Li.

From the set of single scattering events, those with one charged particle outgoing from the carbon analyzer were selected. The vertex in carbon, as well as the angles of the rescattered particle $\theta_{\rm C}$ and $\phi_{\rm C}$, were determined.

Cuts were applied on the vertex in carbon on $\Delta\theta_{\rm C}$ as well as for the $\Delta\phi_{\rm C}$ and ϕ mirror symmetry conditions [44]. The remaining events at all energies represented about 2% of the selected single scattering events.

From the first- and second-scattering vertices, the energy losses in the various materials along the path of the particle were calculated and gave the second-vertex energy T_2. The T_2 and $\theta_{\rm C}$ values were used to determine the corresponding $A_{\rm C}$ value for each accepted event.

The proton–carbon asymmetry was measured for only one outgoing charged particle. The p–C analyzing power $A_{\rm C}$ for this reaction was interpolated from existing results. This procedure is discussed in detail in our preceding paper [39], where an exhaustive list of relevant references is given that we omit here. The interpolated $A_{\rm C}$ values introduce a relative error of ±6% in the rescattering observables at all energies. These observables were determined using the method first proposed by the Geneva group [49]; see also [50].

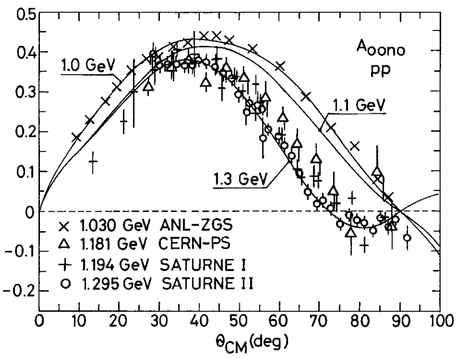

Fig. 7. A_{oono}(pp) energy dependence at three energies. The curves are SG-PSA fits at 1.0, 1.1, and 1.3 GeV. ×: 1.03 GeV ANL [26]; △: 1.181 GeV CERN [24]; +: 1.194 GeV Saturne I [21]; ∘: Saturne II 1.295 GeV [12]

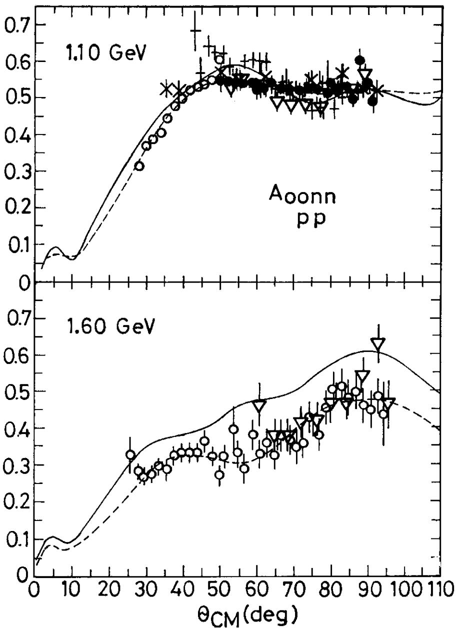

Fig. 8. A_{oonn}(pp) energy dependence at 1.095 and 1.595 GeV. •: protons scattered on H in the ^{6}LiH target; ▽: protons on $^6\mathrm{Li}+\mathrm{D}$ (+H) in the ^{6}LiD target; +: [11]; ∘: [34]; ×: [30]; solid curves: VPI-PSA; dashed curves: SG-PSA

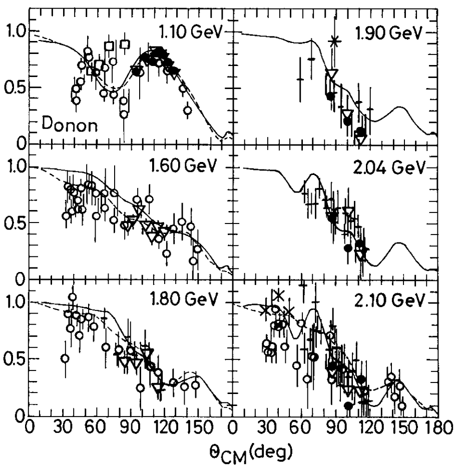

Fig. 9. $D_{\mathrm{onon}}(\theta_{\mathrm{CM}}) = K_{\mathrm{onno}}(180^\circ - \theta_{\mathrm{CM}})$ energy dependence at 1.095, 1.595, 1.795, 1.895, 2.035, and 2.095 GeV. •: protons scattered on H in the ^{6}LiH target (K_{onno}); ▽: protons on $^6\mathrm{Li}+\mathrm{D}$ (+H) in the ^{6}LiD target (K_{onno}); open squares: D_{onon} measured with the ^{6}LiH target; ∘: [36-38]; +: [9,39]; ⋆: BNL 1.90 GeV [40]; ×: 2.205 GeV ANL [41]; solid curves: VPI-PSA; dashed curves: SG-PSA

Table 5. The observable D_{onon} for elastic scattering of polarized protons on the polarized ^{6}LiH target. The relative normalization systematic error in the target polarization was ±4%. The relative systematic error provided by the normalization uncertainty in the p–C analyzing power was ±6%. Another absolute error of ±15% is due to the relative normalization of measurements with the two opposite (and small) P_{T} values

$T_{\mathrm{kin}} = 1.095$ GeV, $p_{\mathrm{lab}} = 1.804$ GeV/c			
θ_{CM} (deg)	Interval (CM deg)	–t (mean) (GeV/c)^2	D_{onon}(pp) H
55.3	51.0–59.0	0.443	0.642 ± 0.079
62.6	59.0–66.0	0.554	0.694 ± 0.087
70.3	66.0–75.0	0.681	0.884 ± 0.101
83.2	75.0–92.0	0.906	0.904 ± 0.097

The CH_2 target, downstream from the polarized target, measured pp single scattering on free protons and on protons in carbon nuclei. The triggers for pp scattering events from the CH_2 target were independent from those used for the polarized target. Events were recorded by the same apparatus and analyzed using the same criteria as for the pp scattering events.

The simultaneous measurements of scattering on a polarized and an unpolarized target are used to check the normalization of events recorded during two opposite target polarizations. This is necessary because the P_{T} was reversed after several hours of data taking, as compared to the $\vec{P}_{\mathrm{B}}$ flip at every spill.

The CH_2 target provided A_{oono} pp elastic scattering on hydrogen and quasi-elastic scattering on protons in carbon. The same method, as described above, was performed to deduce the pp quasi-elastic scattering on strongly bound carbon protons. The two sets of the results are again statistically independent, but the carbon data are more affected by inelastic reactions than the ^{6}Li data.

7 Results and discussion

The results are given with beam energies corresponding to those at the target centers. Independent data obtained in the elastic scattering of protons on H in ^{6}LiH and in CH_2 targets are listed in the tables. Also, quasi-elastic

Table 6. The observable K_{onno} measured with the polarized proton beam scattered on hydrogen in the ^{6}LiH, protons in ^{6}Li in the same target, or protons of the ^{6}LiD target. This parameter depends on the beam polarization only. The relative normalization systematic error in P_{B} was ±3%, and the error provided by the uncertainty in the p–C analyzing power was ±6%

θ_{CM} (deg)	Interval (CM deg)	–t (mean) $(\mathrm{GeV/c})^2$	K_{onno}(pp) H	K_{onno}(pp) ^{6}Li + D (+H)	K_{onno}(pp) ^{6}Li
T_{kin} = 1.095 GeV, p_{lab} = 1.804 GeV/c					
54.0	49.5–56.0	0.425	0.668 ± 0.035	0.635 ± 0.032	0.558 ± 0.049
57.4	56.0–59.0	0.474	0.727 ± 0.041	0.693 ± 0.036	0.635 ± 0.052
61.0	59.0–63.0	0.529	0.817 ± 0.036	0.802 ± 0.032	0.738 ± 0.048
64.5	63.0–66.0	0.585	0.854 ± 0.041	0.843 ± 0.036	0.741 ± 0.058
68.0	66.0–70.0	0.643	0.809 ± 0.040	0.845 ± 0.035	0.727 ± 0.057
72.5	70.0–75.0	0.718	0.720 ± 0.043	0.794 ± 0.036	0.667 ± 0.060
78.4	75.0–82.0	0.821	0.781 ± 0.042	0.736 ± 0.037	0.752 ± 0.060
86.9	82.0–94.6	0.972	0.665 ± 0.044	0.684 ± 0.040	0.641 ± 0.063
T_{kin} = 1.595 GeV, p_{lab} = 2.353 GeV/c					
63.6	57.4–66.0	0.831		0.427 ± 0.066	
68.1	66.0–70.0	0.938		0.460 ± 0.069	
72.5	70.0–75.0	1.047		0.386 ± 0.069	
77.9	75.0–81.0	1.183		0.458 ± 0.075	
84.0	81.0–87.0	1.340		0.649 ± 0.081	
90.0	87.0–93.0	1.497		0.515 ± 0.081	
96.0	93.0–102.1	1.653		0.478 ± 0.090	
T_{kin} = 1.795 GeV, p_{lab} = 2.567 GeV/c					
67.4	60.7–71.0	1.037		0.228 ± 0.093	
75.5	71.0–80.0	1.262		0.517 ± 0.092	
85.1	80.7–90.0	1.540		0.461 ± 0.093	
96.1	90.0–105.9	1.863		0.466 ± 0.089	
T_{kin} = 1.895 GeV, p_{lab} = 2.674 GeV/c					
68.6	61.8–73.0	1.129	0.110 ± 0.148	0.009 ± 0.251	0.143 ± 0.193
79.0	73.0–85.0	1.439	0.207 ± 0.140	0.277 ± 0.241	0.268 ± 0.206
93.4	85.0–104.0	1.883	0.467 ± 0.125	0.635 ± 0.215	0.669 ± 0.183
T_{kin} = 2.035 GeV, p_{lab} = 2.822 GeV/c					
68.0	60.5–73.0	1.194	0.333 ± 0.148	0.224 ± 0.234	0.376 ± 0.204
78.9	73.0–85.0	1.542	0.272 ± 0.143	0.619 ± 0.224	0.529 ± 0.218
94.0	85.0–104.6	2.043	0.539 ± 0.136	0.549 ± 0.213	0.696 ± 0.195

data on $^6Li + D$ (+H) in the ^{6}LiD target, together with those on ^{6}Li and C, are tabulated. Because of the large amount of results, in several figures, only the H and ^{6}LiD data could be plotted. The quoted errors in the tables and the figures are statistical ones. The relative error of P_{B} was ±3%. The error of P_{T} was ±4% at 1.1 GeV, where the target polarization was measured before and after the data acquisition. Then the exponential decrease of P_{T} as a function of time was correctly calculated. Because of a failure of electric power, only one measurement exists at 1.6 GeV, and the error was estimated to be ±10%.

The predictions of two PSA at all energies are plotted in the figures. The independent data for all observables at 1.1 GeV were included into the SG-PSA with their statistical errors. The SG-PSA at other energies and the VPI-PSA at all energies were carried out with the previously existing data only.

Table 6. (continued)

θ_{CM} (deg)	Interval (CM deg)	–t (mean) $(GeV/c)^2$	$K_{onno}(pp)$ H	$K_{onno}(pp)$ $^6Li + D$ (+H)	$K_{onno}(pp)$ ^6Li
T_{kin} = 2.095 GeV, p_{lab} = 2.885 GeV/c					
67.0	60.5–73.0	1.198	0.324 ± 0.181	0.227 ± 0.123	0.323 ± 0.244
78.3	73.0–84.0	1.567	0.099 ± 0.184	0.220 ± 0.126	0.525 ± 0.255
93.5	84.0–104.3	2.086	0.423 ± 0.172	0.370 ± 0.113	0.461 ± 0.247
T_{kin} = 2.395 GeV, p_{lab} = 3.199 GeV/c					
69.0	60.9–77.0	1.442	0.574 ± 0.120	0.000 ± 0.243	0.365 ± 0.166
90.7	77.0–106.2	2.275	0.582 ± 0.125	0.583 ± 0.237	0.392 ± 0.168

In Table 2 are listed the independent A_{oono} results at all energies measured with the ^{6}LiH and ^{6}LiD targets. Measurements at 1.6 GeV were carried out with the ^{6}LiD target only. All the independent results are plotted in Fig. 2, and the H and ^{6}LiD data are shown in Figs. 3 to 5. A significant part of previously measured SATURNE II data is also plotted. We observe an excellent agreement of elastic and quasi-elastic results. Figure 2 shows that the new data at 1.1 GeV improve considerably the accuracy of the Saclay data set above $\theta_{CM} = 43.4°$ [11].

In Table 3 are given the elastic and quasi-elastic pp data obtained with the CH_2 target. For 1.1 GeV, they are plotted in Fig. 6 together with the PSA predictions.

Note that $A_{oono}(pp)$ in the interval $0° < \theta_{CM} < 90°$ reaches its first minimum at $-t \sim 1.0$ $(GeV/c)^2$. This was observed for all available data up to 200 GeV and described in [51]. Additional examples are given in [52]. Around 1.1 GeV this minimum is close to $\theta_{CM} = 90°$, and A_{oono} as a function of θ_{CM} changes rapidly with energy. For this reason, only the A_{oono} data measured very close to 1.1 GeV are shown in Fig. 2.

The SG-PSA fits to all existing data at 1.0, 1.1, and 1.3 GeV are shown in Fig. 7. The accurate elastic ANL-ZGS results [26] at 1.030 GeV are well described by the fit at 1.0 GeV. The angular dependence is closer to a sinusoidal shape with respect to the fit at 1.1 GeV. Two previous experiments have suggested a strong variation of the A_{oono} angular dependence and even negative A_{oono} values at large angles above 1.1 GeV: the SATURNE I data at 1.194 $\pm$ 0.008 GeV [21], and CERN data at 1.181 ± 0.017 GeV [24]. This has been confirmed by the SATURNE II measurements at 1.295 GeV [12], where the A_{oono} values in the region $75° \leq \theta_{CM} < 90°$ are negative. The former energy dependent SG-PSA [53] described this fact well. Since in the interval around 1.1 GeV, $A_{oono}(pp)$ is very sensitive to small energy variations, the excellent agreement of the independent results suggests that no Glauber-type corrections for the quasi-elastic data are needed.

Up to 1.8 GeV at large angles, the A_{oono} values are close to zero, as can be seen in Fig. 3. The minimum at $-t \sim 1.0$ $(GeV/c)^2$ in ANL-ZGS data sets [25,26,29,30] and in the VPI-PSA predictions is pronounced only above 2.2 GeV. At this energy, the minimal values are positive, and the position of the minimum moves below 60° (see Figs. 4, 5).

The spin-correlation parameter $A_{oonn}(pp)$ results at two energies are listed in Table 4. At 1.1 GeV, the free data were accurately determined using the ^{6}LiH target. The errors are larger for the measurements with the ^{6}LiD target because of the small $|P_T|$ values. The results on ^{6}Li have large errors and were omitted. The data at two energies are plotted in Fig. 8. The new data at 1.1 GeV smoothly connect with the SATURNE II results at small angles [34], and are in good agreement with all ANL-ZGS data at 1.047 Gev [30] and with the previous Saclay data above $\theta_{CM} = 63°$ [11]. Below this angle eight points from [11] differ within two statistical errors. The SG-PSA correctly describes all existing data and is in agreement with the VPI-PSA predictions.

At 1.6 GeV, the two PSA predictions for A_{oonn} differ. The SG-PSA includes the SATURNE II points measured at the same energy. The VPI-PSA is affected by former ANL data at other energies with large uncertainties in energy and in P_B normalizations (see [35]).

The pp rescattering observables D_{onon} and K_{onno} are given in Tables 5 and 6, respectively. The H and ^{6}Li data at six lower energies are presented in Fig. 9 with the equality $K_{onno}(\pi - \theta_{CM}) = D_{onon}(\theta_{CM})$ used. They are compared with the previous SATURNE II data [9,36–39], the BNL point at 1.90 GeV [40], and the three ANL points at 2.205 GeV [41]. We observe a good agreement among all new K_{onno} results plotted at large angles. This quantity depends on the large $|P_B|$ values only. The D_{onon} points at 1.1 GeV, depending on the relatively small P_T values, are more dispersed. Note that the number of events was at least 50 times smaller than for single scattering. We observe a good agreement with the majority of the existing data points and the two PSA predictions. The data at 1.6 and 1.8 GeV were obtained with the ^{6}LiD target only. The ^{6}LiH target was not used at 1.6 GeV. The statistics of K_{onno} events, recorded with this target at 1.8 GeV, was very small and the results were omitted. At 2.4 GeV, only two points with large errors were obtained, and they are listed in Table 6.

8 Conclusions

Quasi-elastic scattering of protons on weakly bound protons in deuterons and in ^{6}Li nuclei shows agreement with elastic scattering results for all measured observables. The equality of elastic and quasi-elastic scattering data suggests that ^{6}LiD is an excellent target for experiments with polarized nucleons. It also suggests that no additional corrections to spin-dependent pp $\rightarrow$ pp data are needed. The quasi-elastic scattering on strongly bound nucleons in carbon nuclei is more dependent on cuts.

The present results at 1.1 GeV improve significantly our knowledge of analyzing power, spin-correlation parameter, and rescattering observable angular dependence. At higher energies, the new data supplement the existing database. Since the pp PSA below 2.4 GeV is still fairly well constrained, the comparison of predictions with the new elastic and quasi-elastic pp results is significant.

Acknowledgements. The SG-PSA fits were carried out with a help of C. Lechanoine-Leluc. We express our gratitude to R.A. Arndt and I.I. Strakovsky for the recent VPI-PSA predictions. We also thank the members of the well-organized SATURNE II operations crew for their help. This work was supported in part by the U.S. Department of Energy, Division of Nuclear Physics, Contract No. W-31-109-ENG-38, by the Swiss National Science Foundation, and by the Russian Foundation for Fundamental Nuclear Physics Programme 122.03.

References

1. C.D. Lac, J. Ball, J. Bystrický, J. Derégel, F. Lehar, A. de Lesquen, L. van Rossum, J.-M. Fontaine, F. Perrot, P. Winternitz, J. Phys. France **51**, 2689 (1990)
2. J. Bystrický, C. Lechanoine-LeLuc, F. Lehar, Eur. Phys. J. C **4**, 607 (1998)
3. J. Ball, J. Bystrický, J.-M. Fontaine, G. Gaillard, R. Hess, Z. Janout, B.A. Khachaturov, R. Kunne, C.D. Lac, C. Lechanoine-Leluc, F. Lehar, A. de Lesquen, D. Lopiano, F. Perrot-Kunne, D. Rapin, L. van Rossum, H. Schmitt, H.M. Spinka, Nuovo Cimento A **111**, 13 (1998)
4. J. Bystrický, C. Lechanoine-Leluc, F. Lehar, J. Phys. France **51**, 2747 (1990)
5. R.A. Arndt, C.H. Oh, I.I. Strakovsky, R.L. Workman, F. Dohrman, Phys. Rev. C **56**, 3005 (1997), SAID solution SP99
6. J. Bystrický, F. Lehar, P. Winternitz, J. Physique (Paris) **39**, 1 (1978)
7. F. Halzen, G.H. Thomas, Phys. Rev. D **10**, 344 (1974)
8. I.P. Auer, J. Chalmers, E. Colton, R. Giese, H. Halpern, D. Hill, R. Miller, K. Nield, B. Sandler, H. Spinka, N. Tamura, D. Underwood, Y. Watanabe, A. Yokosawa, A. Beretvas, D. Miller, Phys. Rev. D **32**, 1609 (1985)
9. C.E. Allgower, J. Ball, L.S. Barabash, M. Beddo, Y. Bedfer, A. Boutefnouchet, J. Bystrický, P.-A. Chamouard, Ph. Demierre, J.-M. Fontaine, V. Ghazikhanian, D. Grosnick, R. Hess, Z. Janout, Z.F. Janout, V.A. Kalinnikov, T.E. Kasprzyk, Yu.M. Kazarinov, B.A. Khachaturov, R. Kunne, C. Lechanoine-LeLuc, F. Lehar, A. de Lesquen, D. Lopiano, M. de Mali, V.N. Matafonov, I.L. Pisarev, A.A. Popov, A.N. Prokofiev, D. Rapin, J.-L. Sans, H.M. Spinka, Yu.A. Usov, V.V. Vikhrov, B. Vuaridel, C.A. Whitten, A.A. Zhdanov, Eur. Phys. J. C **5**, 453 (1998)
10. Ch. Allgower, J. Arvieux, P. Ausset, J. Ball, P.-Y. Beauvais, Y. Bedfer, J. Bystrický, P.-A. Chamouard, Ph. Demiere, J.-M. Fontaine, Z. Janout, V.A. Kalinnikov, T.E. Kasprzyk, B.A. Khachaturov, R. Kunne, J.-M. Lagniel, F. Lehar, A. de Lesquen, A.A. Popov, A.N. Prokofiev, D. Rapin, J.-L. Sans, H.M. Spinka, A. Teglia, V.V. Vikhrov, A.A. Zhdanov, Nucl.Instrum.Methods A **399**, 171 (1997)
11. J. Bystrický, P. Chaumette, J. Derégel, J. Fabre, F. Lehar, A. de Lesquen, F. Petit, L. van Rossum, J.-M. Fontaine, F. Perrot, J. Ball, A. Michalowicz, Y. Onel, A. Penzo, Nucl. Phys. B **262**, 715 (1985)
12. F. Perrot, J.-M. Fontaine, F. Lehar, A. de Lesquen, J.P. Meyer, L. van Rossum, P. Chaumette, J. Derégel, J. Fabre, J. Ball, C.D. Lac, A. Michalowicz, Y. Onel, B. Aas, D. Adams, J. Bystrický, V. Ghazikhanian, G. Igo, F. Sperisen, C.A. Whitten, A. Penzo, Nucl. Phys. B **294**, 1001 (1987)
13. C.E. Allgower, J. Ball, M. Beddo, Y. Bedfer, A. Boutefnouchet, J. Bystrický, P.-A. Chamouard, Ph. Demierre, J.-M. Fontaine, V. Ghazikhanian, D. Grosnick, R. Hess, Z. Janout, Z.F. Janout, V.A. Kalinnikov, T.E. Kasprzyk, B.A. Khachaturov, R. Kunne, F. Lehar, A. de Lesquen, D. Lopiano, V.N. Matafonov, I.L. Pisarev, A.A. Popov, A.N. Prokofiev, D. Rapin, J.-L. Sans, H.M. Spinka, A. Teglia, Yu.A. Usov, V.V. Vikhrov, B. Vuaridel, C.A. Whitten, and A.A. Zhdanov, Nucl. Phys. A **637**, 231 (1998)
14. J. Arvieux, J. Ball, J. Bystrický, J.-M. Fontaine, G. Gaillard, J.P. Goudour, R. Hess, R. Kunne, F. Lehar, A. de Lesquen, D. Lopiano, M. de Mali, F. Perrot-Kunne, D. Rapin, L. van Rossum, J.-L. Sans, and H.M. Spinka, Zeitschrift für Physik C **76**, 465 (1997)
15. J. Ball, M. Beddo, Y. Bedfer, J. Bystrický, P.-A. Chamouard, M. Combet, Ph. Demierre, J.-M. Fontaine, G. Gaillard, D. Grosnick, R. Hess, R. Kunne, F.Lehar, A. de Lesquen, D. Lopiano, D. Rapin, J.-L. Sans, H.M. Spinka, Eur. Phys. J. C DOI 10.1007/s100529900109 (in press)
16. J. Ball, V. Ghazikhanian, J. Gordon, F. Lehar, A. de Lesquen, F. Perrot, L. van Rossum, Nucl. Phys. B **286** (1987) 635
17. C.E. Allgower, Ph.D. thesis, ANL-HEP-TR-97-71, August 1997
18. M. Garçon, J.C. Duchazeaubeinex, J.C. Faivre, B. Guillerminet, D. Legrand, M. Rouger, J. Saudinos, J. Arvieux, Phys. Lett. B **183**, 273 (1987)
19. S. Dalla Torre-Colautti, R. Birsa, F. Bradamante, M. Giorgi, L. Lanceri, A. Martin, A. Penzo, P. Shiavon, V. Sossi, A. Villari, H. Azaiez, K. Kuroda, A. Michalowicz, F. Lehar, Nucl. Phys. A **505**, 561 (1989)
20. P. Bareyre, J.F. Detoeuf, L.W. Smith, R.D. Tripp, L. van Rossum, Nuovo Cimento **20**, 1049 (1961)
21. G. Cozzika, Y. Ducros, A. de Lesquen, J. Movchet, J.C. Raoul, L. van Rossum, J. Derégel, J.-M. Fontaine, Phys.Rev. **164**, 1672 (1967)
22. H.A. Neal, M.J. Longo, Phys. Rev. **161**, 1374 (1967)
23. P. Grannis, J. Arens, F. Betz, O. Chamberlain, B. Dieterle, C. Schultz, G. Shapiro, L. van Rossum, D. Weldon, Phys. Rev. **148**, 1297 (1966)

24. M.G. Albrow, S. Andersson/Almehed, B. Bosniakovic, C. Daum, F.C. Erne, J.P. Lagnaux, J.C. Sens, F. Udo, Nucl. Phys. B **23**, 445 (1970)
25. V.V. Zhurkin, I.M. Ivanchenko, V.P. Kanavets, N.N. Karpenko, I.I. Levintov, V.I. Martynov, O.E. Mikhailov, B.V. Morozov, V.M. Nesterov, I.I. Pershin, L.M. Polyakova, V.V. Ryltsov, T.S. Cherkalina, Yad. Fiz. **28** (1978) 1280 and Sov. J. Nucl. Phys **28**, 660 (1978)
26. M.L. Marshak, E.A. Peterson, K. Ruddick, J. Lesikar, T. Mulera, J.B. Roberts, R.D. Klem, R. Talaga, A. Wriekat, Phys. Rev. C **18**, 331 (1978)
27. D. Miller, C. Wilson, R. Giese, D. Hill, K. Nield, P. Rynes, B. Sandler, A. Yokosawa, Phys. Rev. D **16**, 2016 (1977)
28. J.H. Parry, N.E. Booth, G. Conforto, R.J. Esterling, J. Scheid, D.J. Sherden, and A. Yokosawa, Phys. Rev. D **8**, 45 (1973)
29. A. Lin, J.R. O'Fallon, L.G. Ratner, P.F. Schultz, K. Abe, D.G. Crabb, R.C. Fernow, A.D. Krisch, A.J. Salthouse, B. Sandler, K.M. Terwilliger, Phys. Lett. **74B**, 273 (1978)
30. D.A. Bell, J.A. Buchanan, M.M. Calkin, J.M. Clement, W.H. Dragoset, M. Furič, K.A. Johns, J.D. Lesikar, H.E. Miettinen, T.A. Mulera, G.S. Mutchler, G.G. Phillips, J.B. Roberts, S.E. Turpin, Phys. Lett. **94B**, 310 (1980)
31. Y. Makdisi, M.L. Marshak, B. Mossberg, E.A. Peterson K. Ruddick, J.B. Roberts, R.D. Klem, Phys. Rev. Lett. **45**, 1529 (1980) The numerical values are in the thesis of Björn Mossberg from University of Minnesota
32. R. Diebold, D.S. Ayres, S.L. Kramer, A.J. Pawlicki, A.B. Wicklund, Phys. Rev. Lett. **35**, 632 (1975)
33. Y. Kobayashi, K. Kobayashi, T. Nakagawa, H. Shimizu, H.Y. Yoshida, H. Ohnuma, J.A. Holt, G. Glass, J.C. Hiebert, R.A. Kenefick, S.Nath, L.C. Northcliffe, A.J. Simon, S. Hiramatsu, Y. Mori, H. Sato, A. Takagi, T. Toyama, A. Ueno, K. Imai, Nucl. Phys. A **569**, 791 (1994)
34. F. Lehar, A. de Lesquen, J.P. Meyer, L. van Rossum, P. Chaumette, J. Derégel, J. Fabre, J.-M. Fontaine, F. Perrot, J. Ball, C.D. Lac, A. Michalowicz, Y. Onel, D. Adams, J. Bystrický, V. Ghazikhanian, C.A. Whitten, A. Penzo, Nucl. Phys. B **294** (1987) 1013
35. H. Spinka, E. Colton, W.R. Ditzler, H. Halpern, K. Imai, R. Stanek, N. Tamura, G. Theodosiou, K. Toshioka, D. Underwood, R. Wagner, Y. Watanabe, A. Yokosawa, G.R. Burleson, W.B. Cottingame, S.J. Greene, S. Stuart, J.J. Jarmer, Nucl. Instrum. Methods **211**, 239 (1983)
36. C.D. Lac, J. Ball, J.Bystrický, F. Lehar, A. de Lesquen, L. van Rossum, F. Perrot, J.-M. Fontaine, P. Chaumette, J. Derégel, J. Fabre, V. Ghazikhanian, A. Michalowicz, Nucl. Phys. B **321**, 284 (1989)
37. C.D. Lac, J. Ball, J. Bystrický, F. Lehar, A. de Lesquen, L. van Rossum, F. Perrot, J.-M.Fontaine, P. Chaumette, J. Derégel, J. Fabre, V. Ghazikhanian, A. Michalowicz, Y. Onel, A. Penzo, Nucl. Phys. B **315**, 284 (1989)
38. C.D. Lac, J. Ball, J. Bystrický, F. Lehar, A. de Lesquen, L. van Rossum, F. Perrot, J.-M. Fontaine, P. Chaumette, J. Derégel, J. Fabre, V. Ghazikhanian, A. Michalowicz, Nucl. Phys. B **321**, 269 (1989)
39. C.E. Allgower, J. Ball, L.S. Barabash, M. Beddo, Y. Bedfer, A. Boutefnouchet, J. Bystrický, Ph. Demierre, J.-M. Fontaine, V. Ghazikhanian, D. Grosnick, R. Hess, Z. Janout, Z.F. Janout, V.A. Kalinnikov, T.E. Kasprzyk, Yu.M. Kazarinov, B.A.Khachaturov, R. Kunne, F. Lehar, A. de Lesquen, D. Lopiano, M. de Mali, V.N. Matafonov, I.L. Pisarev, A.A. Popov, A.N. Prokofiev, D. Rapin, J.-L. Sans, H.M. Spinka, S. Trentalange, Yu.A. Usov, V.V. Vikhrov, B. Vuaridel, C.A. Whitten, A.A. Zhdanov, Eur. Phys. J. C **1**, 131 (1998)
40. W.C. Carithers, Jr., R.K. Adair, C.J.B. Hawkins, H. Kasha, R.C. Larsen, L.B. Leipuner, L.W. Smith, T.P. Wangler, Phys. Rev. **179**, 1304 (1969)
41. G.W. Abshire, G.W. Bryant, M. Corcoran, R.R. Crittenden, S.W. Gray, R.M. Heinz, A.W. Hendry, H.A. Neal, D.R. Rust, Phys. Rev. D **12**, 3393 (1975)
42. J. Bystrický, J. Derégel, F. Lehar, A. de Lesquen, L. van Rossum, J.-M. Fontaine, F. Perrot, C.A. Whitten, T. Hasegawa, C.R. Newsom, W.R. Leo, Y. Onel, S. Dalla Torre-Colautti, A. Penzo, H. Azaiez, and A. Michalowicz, Nucl. Instrum. Methods A **239**, 131 (1985)
43. M. Arignon, J. Bystrický, J. Derégel, J.-M. Fontaine, T. Hasegawa, F. Lehar, C.R. Newsom, A. Penzo, F. Perrot, L. van Rossum, C.A. Whitten, and J. Yonnet, Note CEA-N-2375, Saclay, Décembre 1983
44. J. Ball, Ph. Chesny, M. Combet, J.-M. Fontaine, R. Kunne, J.-L. Sans, J. Bystrický, C.D. Lac, D. Legrand, F. Lehar, A. de Lesquen, M. de Mali, F. Perrot-Kunne, L. van Rossum, P. Bach, Ph. Demierre, G. Gaillard, R. Hess, Z.F. Janout, D. Rapin, Ph. Sormani, B. Vuaridel, J.P. Goudour, R. Binz, A. Klett, E. Rössle, H. Schmitt, L.S. Barabash, Z. Janout, V.A. Kalinnikov, Yu.M. Kazarinov, B.A. Khachaturov, V.N. Matafonov, I.L. Pisarev, A.A. Popov, Yu.A. Usov, M. Beddo, D. Grosnick, T. Kasprzyk, D. Lopiano, H. Spinka, Nucl. Instrum. Methods A **327**, 308 (1993)
45. S. Ritt, E.T. Boschitz, R. Meier, R. Tacik, M. Wessler, K. Junker, J.A. Konter, S. Mango, D. Renker, B. van den Brandt, V. Efimovykh, A. Kovaljov, A. Prokofiev, R. Mach, P. Chaumette, J. Derégel, G. Durand, J. Fabre, W. Thiel, Phys. Rev. C **43**, 745 (1991)
46. S. Bültmann, D.G. Crabb, D.B. Day, R.D. Fatemi, B. Gardner, C.M. Harris, J.R. Johnston, J.S. McCarthy, P.M. McKee, W. Meyer, S.I. Pentillä, E. Ponikvar, A. Rijllart, O.A. Rondon, S. St. Lorant, W.A. Tobias, S. Trentalange, H. Zhu, B. Zihlmann, D. Zimmermann, A Study of Lithium Deuteride as a Material for a Polarized Target, Preprint SLAC-PUB-7904, August 1998 (to be published)
47. J. Ball, M. Combet, J.-L. Sans, B. Benda, P. Chaumette, J. Derégel, G. Durand, A.P. Dzyubak, C. Gaudron, F. Lehar, A. de Lesquen, T.E. Kasprzyk, Z. Janout, B.A. Khachaturov, V.N. Matafonov, Yu.A. Usov, Nucl. Instrum. Methods A **381**, 4 (1996)
48. St. Goertz, Ch. Bradtke, H. Dutz, R. Gehring, W. Meyer, M. Plückthun, G. Reicherz, K.Runkel, A. Thomas, Nucl. Instrum. Methods A **356**, 20 (1995)
49. D. Besset, Q.H. Do, B. Favier, L.G. Greeniaus, R. Hess, C. Lechanoine, D. Rapin, D.W. Werren, Ch. Weddigen, Nucl. Instrum. Methods **166**, 379 (1979)
50. A. Teglia, Ph.D. Thèse No 2948, DPNC, Université de Genève, 1997
51. F.Lehar, A. de Lesquen, F. Perrot, L. van Rossum, Europhysics Lett. **3**, 1175 (1987)
52. C. Lechanoine-Leluc, F. Lehar, Rev. Mod. Phys. **65**, 47 (1993)
53. F. Lehar, C. Lechanoine-Leluc, J. Bystrický, J. Physique (Paris) **48**, 1273 (1987)